Inspection of Ball Grid Array(BGA) Solder Joints using X-ray Cross-sectional Images

Y.J. Roh[a], K.W. Ko[a], H.S. Cho[a],
H.C Kim[b], H.N. Joo[b], S.K. Kim[b]

[a]Dept. of Mechanical Eng., Korea Advanced Institute of Science and Technology
[b]FA Research Institute Production Engineering Center, Samsung Electroncs Co., LTD

ABSTRACT

The ball grid array(BGA) chip is widely used in high density printed circuit board(PCB). However, inspection of defects in the solder joints is difficult by visual or a normal x-ray imaging method, because unlike conventional packages with gull-wing type leads, solder joints of the BGA are located underneath its own package and ball type leads. Therefore, x-ray digital tomosynthesis(DT), which form a cross-sectional image of 3-D objects, is needed to image and inspect the solder joints of BGA. In this paper, we propose a series of algorithms for inspecting the solder joints of BGA by using x-ray cross-sectional images that are acquired from the developed DT system. BGA solder joints are examined to check the alignment between the chip and pad on a PCB, bridge(electrically short), adequate solder volume. The volume of the solder joint is represented by a gray level in the x-ray images : thus solder joints can be examined by use of the gray-level profiles of each joint. To inspect and classify various defects, pattern classification method using a learning vector quantization(LVQ) neural network and a look up table(LUT) is proposed. The clusters into which a gray-level profile is classified are generated by the learning process of the network by using a number of sampled gray-level profiles. A series of these developed algorithms for inspecting and classifying defects were tested on a number of BGA solder joints. The experimental results show that the proposed method yields satisfactory solutions for inspection based on x-ray cross-sectional images.

Keywords : x-ray cross-sectional image, digital tomosynthesis, solder joint inspection, BGA, neural network.

1. INTRODUCTION

The Ball Grid Array(BGA) chips are widely used these days due to its high efficiency in making high-density printed circuit boards(PCB). However, from the point of view of quality inspection, it is very difficult to inspect them visually or with a normal x-ray imaging method (x-ray radiography), because unlike the conventional packages with gull-wing type leads on the sides them, solder joints of BGA are located underneath its own package and ball type leads[1-4]. Figure 1 illustrates a BGA package and an x-ray radiography image of a PCB with a BGA chip. In the x-ray image, it is difficult to discern the solder joints of the BGA, since they are imaged together with the ball lead and the solder joints on the other side of the PCB. Therefore x-ray cross-sectional imaging methods such as laminography and digital tomosynthesis (DT), which can form a cross-sectional images of 3-D objects, is needed to image and inspect the BGA solder joints. From the cross-sectional images, we can see the solder joint and inspection algorithms to check the joint quality can be applied. However the images does not show the exact cross-section of the joints, since there can be an artifact or blurring effects by the materials out of the focal plane[5-6]. Therefore, it is not easy to separate the solder joints perfectly in the images. For this reason, conventional inspection methods using geometrical features such as diameter, area extracted from gray-level images often yield unsatisfactory solution[1]. In this paper, to avoid such criticism, the patterns of intensity distribution for solder joints are used as features determining the solder joint quality. Considering the number of data processed, the intensity distribution is represented by several intensity profiles. By using LVQ neural network the profiles are classified into several

Further author information -

H.S. Cho : E-mail : hscho@lca.kaist.ac.kr ; URL : http://lca.kaist.ac.kr/~hscho; Telephone : +82-42-869-3213; Fax : +82-42-869-3210

Part of the SPIE Conference on Machine Vision Systems for Inspection and Metrology VIII • Boston, Massachusetts • September 1999
SPIE Vol. 3836 • 0277-786X/99/$10.00

groups, and the classification results are used to determine solder joint quality based on the rule defined in a LUT. To evaluate the classification performance of the proposed method, a series of experiments were conducted with various BGA solder joints of commercially manufactured PCBs. The experimental results show practical usefulness of the proposed method for solder joint inspection.

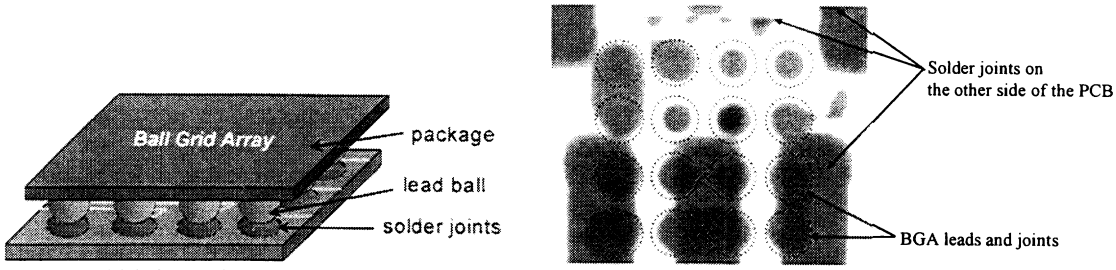

(a) BGA package (b) An x-ray radiography image

Figure 1. BGA package and an x-ray radiograph image of a PCB

2. X-ray Cross-sectional imaging system

2.1 The principle of x-ray cross-sectional imaging method

Laminography, which was originated by Bocage[7], is one method for acquiring cross-sectional images and has been used for years in both medicinal and engineering area to see through opaque materials to find the underlying material's structure. Its principle comes from the geometric focusing effect of the synchronized motion between an x-ray source and a detector, as shown in figure 2.

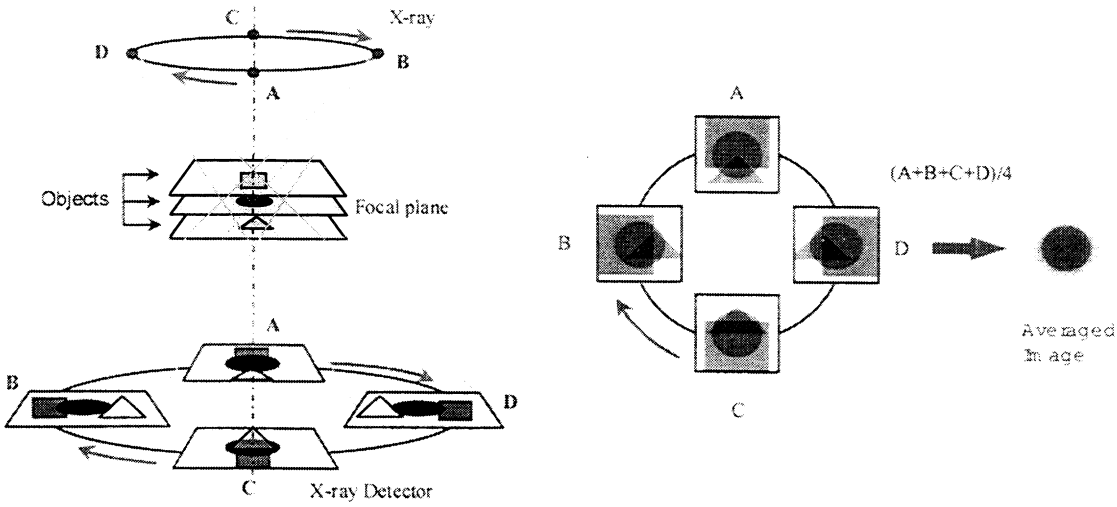

(a) Principle of laminography (b) Projected images and a cross-sectional image

Figure 2. The principle of Laminography and DT

A rotating x-ray source and an image detector with respect to a same axis generate a geometrical focal plane. As the figure 2 shows, the circular object on the focal plane is imaged at the same position, whereas the other objects outside the focal plane are projected at different positions as the x-ray projects the objects with different views. Thus, averaging those images projected from different views has the effect to eliminate the out of focal plane objects in the image preserving the images on the focal plane.

2.2 Digital tomosynthesis imaging system

Figure 3 shows the structure of the developed DT system, which consists of a scanning x-ray tube, an image intensifier, a rotating prism and a camera equipped with a zoom lens. The scanning x-ray tube is designed to electrically control the position of an x-ray spot, and to project an x-ray beam into an object (PCB) from different directions. Attenuated x-rays passing through the PCB are collected by an image intensifier, and converted into a visible image on the instrument's output screen.

The region of interest of the PCB is projected on a circular trajectory on the image intensifier as the x-ray is steered, and eight or more images are sequentially acquired by the zoom camera through the rotating prism. The prism rotate in synchronization with the x-ray position to capture the projected images on the screen of image intensifier as shown in figure 3 (b). The images captured at different positions are saved in the digital memory of a computer, and then averaged to generate a cross-sectional image of the focal plane. Practically, an image correction process is needed before synthesizing the images, as the curved input surface of the image intensifier distorts the image[8-10].

The x-ray imaging conditions in the system, such as the projection angle and the magnification, are determined by the geometric relations of the parameters ; these are the radius of the rotating x-ray and the distances from the x-ray to the object plane and to the surface of the image intensifier. The projection angle is an important parameter in the DT system, since the artifact that causes distortions of the cross-section in the resulting image can generally be reduced or removed as the projection angle increases[1-2, 5-6]. In the developed x-ray imaging system, the incident angle for BGA solder joint inspection is set to about 30 degree. All the processes including the x-ray, prism control and synthesizing of the 8 images requires 400ms to acquire a cross-section image.

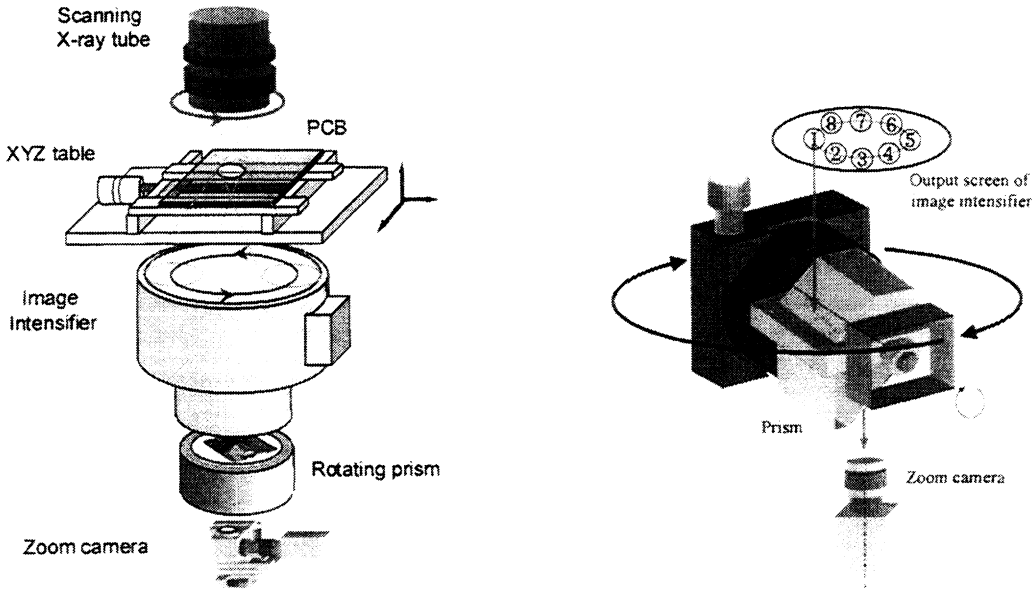

(a) A schematic of the developed system (b) Local images acquisition by a rotating prism

Figure 3. The structure of the developed digital tomosynthesis system

2.3 The cross-sectional image of BGA solder joints

The schematic diagram of a BGA and cross-sectional images at three differently located focal planes is shown in figure 4. The focal planes are changed from the ball-center(A) to the solder joint part(C) that is close to the pad. For the BGA solder joints inspection, the x-ray images for the focal plane C were used.

Figure 4 (b) shows the experimental x-ray images acquired by the developed DT system. In the image of plane A, the balls have the largest diameter and there are no artifact. But as the focal plane departs from the plane of A, the diameters of the balls are imaged as smaller ones and the blurring effects are shown in the images.

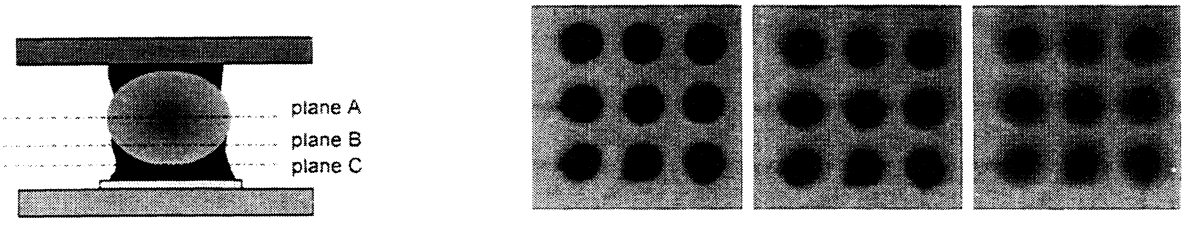

(a) Three planes for cross-section (b) Cross-sectional images

Figure 4. The cross-sectional images of three different planes of BGA

X-ray cross-sectional image of the BGA solder joint from laminography or the DT method has an inherent blurring effect and artifact as shown in figure 4. The blurs in the image is come from the afterimage of eliminated ball leads, but the information on the solder joint can also be included within the blurred area. This problem has been a major obstacle to extract suitable geometric features of the solder joint for classification. Therefore, an inspection algorithm is needed which considers the patterns of the intensity distribution of solder joints in x-ray images.

3. BGA solder joints inspection

3.1 checking mis-location of the solder ball

The first step of the inspection is to check the location error of the solder joints. It is supposed that the locations of the pads in a x-ray image are predetermined by the teaching process and CAD data of the PCB. Each ball lead can be mislocated with respect to the pad on the PCB as shown in figure 5 due to improper soldering conditions such as disturbing external force or unusual heating time and temperature[10].

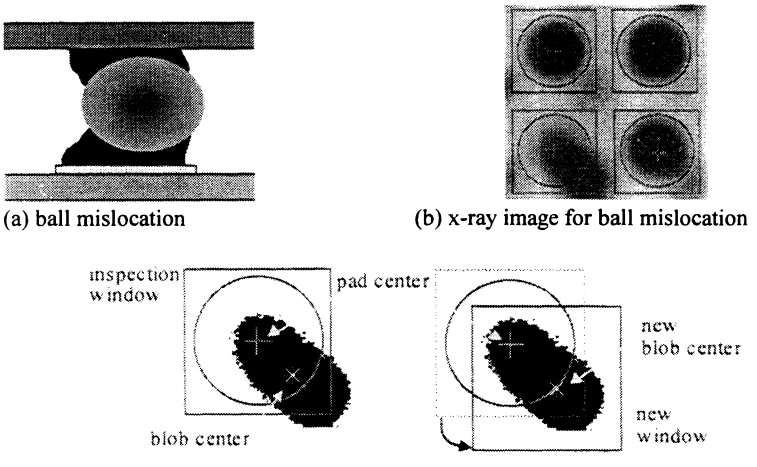

(a) ball mislocation (b) x-ray image for ball mislocation

(c) moving window process

Figure 5. Ball misalignment checking algorithm

When a ball lead is located off-center, the joint image for the focal plane is eccentrically shaped. The distance between the predetermined pad center and the ball center in the image is defined as offset of the ball lead, and can be evaluated by blob analysis in the binarized image. When a joint has a large offset value, it cannot be wholly included within the predetermined inspection window, as shown in figure 5 (b). Considering this case, a moving window process is needed ; this is graphically explained in figure 5 (c). The maximum acceptable offset displacement can be defined arbitrarily by experts ; we set the reasonable threshold value as 15% of the ball diameter in the image.

3.2 Checking the bridge between solder joints

Among the various defects in solder joints, solder bridge (undesirable connections between two or more joints) is the most serious defect, since it can directly result in the functional disorder of products. To inspect and locate the solder bridge between ball joints, four searching windows surrounding a joint are placed as shown in figure 6. The bridge checking algorithm is performed on binarized image by searching for the presence of a line across the joints. Moving the line mask along the searching direction illustrated at figure 6(b) with binary AND operation can report on the width of the bridge.

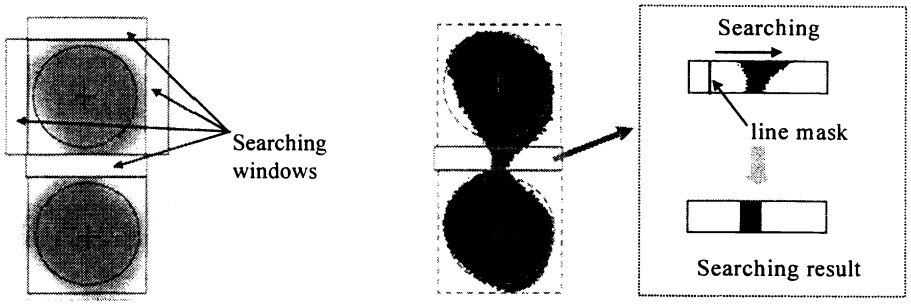

(a) searching windows (b) bridge checking in binary image

Figure. 6 Solder bridge checking method

3.3 Solder volume inspection using intensity profiles

The quality of solder volume (adequacy, insufficiency or excess) for each joint can be evaluated from the intensity distribution in the cross-section images. DT cross-section images do not correctly represent the cross-sections of the joints, since artifacts and blur effects are included in the image by materials out of the focal plane. However, the cross-section image for the plane of the solder joints can indicate the solder volume state if there is some distortion in the cross-section. The intensity distribution of the joints in the image is used to discriminate defects in the solder joint. Rather than considering all the intensity values, four gray level profiles along the lines passing through the center of a joint in an image(figure 7) are used to reduce data size and computation time.

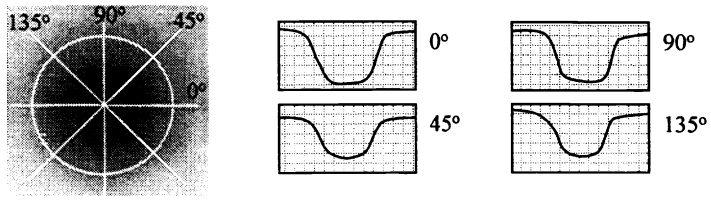

Figure 7. Four gray level profiles to be examined

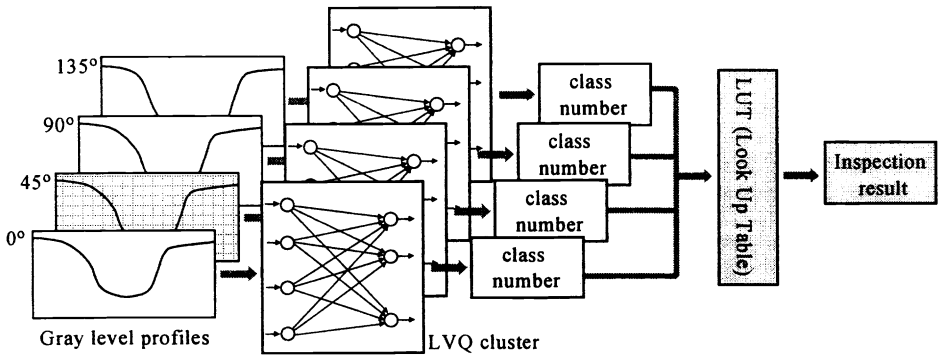

Figure 8. Solder volume inspection process

The solder volume inspection method is shown as figure 8. The four directional gray level profiles of a joint are classified by the same number of LVQ neural networks, and the its classification results are used as an input element for the look up table(LUT) that determines the state of the solder volume. The LVQ neural network can cluster gray-level profiles into several groups which can be understood as solder joint qualities.

3.4 LVQ neural network for clustering intensity profiles

The learning vector quantization neural network is a well-known unsupervised neural network for clustering and data compression. Clustering involves grouping similar patterns and separating dissimilar patterns with no priori information[11-14]. In our research, LVQ network is used for clustering input gray-level profiles with several number of groups according to their similarities, and it plays a role of a preprocessor. The network consists of an input layer and an output layer as shown in figure 9. Every nodes in the input layer are connected directly to the neurons in the output layer. A weight vector called as a prototype vector is associated with each neuron in the output layer. During the learning process, the weights between the neurons are updated so as to resemble each input data. In the self-clustering procedure, the output nodes compete with each other by measuring similarities between an input vector and the weight vectors that are connected to the output neurons. Then just one output neuron, whose weight vector closest to the current input data, is selected as a winner. And only the weights of the winner output node are qualified to be updated, so that the weights approach the members grouped in the cluster. This learning method is the well known and widely used competitive learning rule or the winner take all[11].

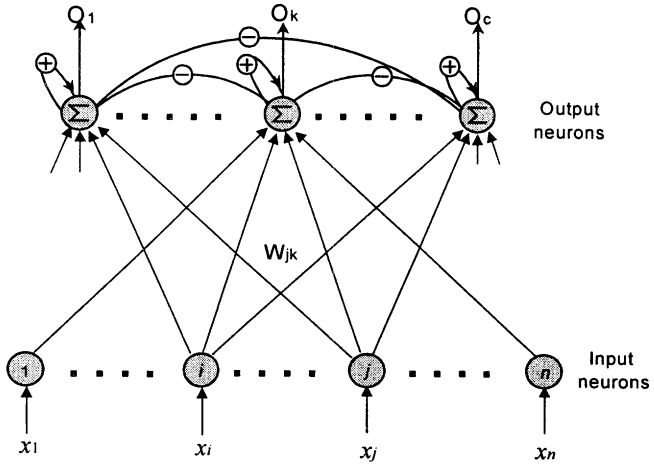

Figure 9. LVQ (learning vector quantization) neural network structure

The training of the LVQ neural network is executed as follows. Let $\vec{X}$ and $\vec{W}$ be input and weight vectors respectively, the output of the neuron in the competitive layer is calculated by equation (1) where N_c is the number of output neurons.

$$d_i = \left\| \vec{X} - \vec{W}_i \right\|^2, \quad i = 1,2,\cdots,N_c \tag{1}$$

The weight vector is updated by the equation (2) where $\alpha(t)$ is the dynamic learning rate, which decrease as t increases.

$$\vec{W}_i(t+1) = \begin{cases} \vec{W}_i(t) + \alpha(t) \cdot (\vec{X}(t) - \vec{W}_i(t)), & \text{if } \arg\min_i d_i \\ \vec{W}_i(t), & \text{otherwise} \end{cases} \tag{2}$$

The input of the LVQ neural network is the gray-level profile in the cross-sectional image of the BGA. Thus the number of neurons in the input layer corresponds to the pixel number on a line mask to sample the intensity profile in x-ray image. The number of neurons in the competitive layer is the same as the cluster number.

3.5 Optimal class number in LVQ network

The LVQ network is a useful tool for classification problems with simple learning methods and fast convergence. However, it is difficult to determine the optimal number of output nodes. To find this for practical applications, various experiments with changing numbers of output neurons are executed. Then a fitness index representing the performance of the classification is proposed in this study, by using the fitness value we can determine the optimal number of output nodes in the LVQ network.

The classification performance can be evaluated by two criteria. The first is the similarity between a prototype and the patterns belonging to it ; it can be measured by the averaged distances δ_i as formulated in equation (3). In equation (3) n_i is the number of input patterns that is classified into class i , $\mathbf{P}^i$ is a prototype vector of the class i and $\mathbf{X}^i_k$ is k_{th} input patterns belonging to the class.

$$\delta_i = \frac{1}{n_i}\sum_{k=1}^{n_i}\left\|\mathbf{P}^i - \mathbf{X}^i_k\right\| \tag{3}$$

The second criterion is the dissimilarity between prototypes that are the representatives of the classes; this can also be measured by the averaged distances D_i of a prototype to the others as shown in equation (4). In this equation, N_c is the number of output nodes (class number), $\mathbf{P}^i$ and $\mathbf{P}^j$ are i_{th} and j_{th} prototype vectors respectively.

$$D_i = \frac{1}{N_c}\sum_{j=1, j\neq i}^{N_c}\left\|\mathbf{P}^i - \mathbf{P}^j\right\| \tag{4}$$

Thus considering the two terms together, we evaluate the performance of the classification with a fitness index F formulated by equation (5). In the equation f_i is the fitness value for the i_{th} class. As a result, a small value of F reports that the classification is well processed with a suitable number of classes.

$$F = \frac{1}{N_c}\sum_{i=1}^{N_c} f_i = \frac{1}{N_c}\sum_{i=1}^{N_c}\frac{\delta_i}{D_i} \tag{5}$$

4. Experimental results and discussions

4.1 Experimental conditions

The developed inspection algorithms were tested on DT images of BGA samples that included various types of defects such as solder bridge, ball misalignment, and solder volume defects. The sample images were acquired by the developed DT system ; the imaging conditions are listed in Table 1.

X-ray view angle	28 (degree)
Synthesizing image number	8 (images)
Geometric magnification	4.5
Image resolution	400 x 400 (pixel)
Field of view size	6 x 6 (mm)
X-ray power	110kV, 0.2mA

Table 1. X-ray DT imaging conditions

The sample images include 126 BGA solder joints. From this sample, 58 randomly selected joints were used for network training, and the remaining 68 joints were used for testing. Practically, four profiles are extracted from each joint and used in the training, the number of input data were 232. For feasibility tests on the algorithm, all samples were also grouped by an expert inspector into three classes according to their qualities : insufficient soldering (*I*), acceptable soldering (*A*), and excessive soldering (*E*).

4.2 Training of LVQ clustering network

The input of the LVQ clustering network is gray-level profile data sampled from the BGA image, as illustrated in figure 7. The number of input node was set to 100 ; the initial dynamic learning rate was set to 0.3 and decreased to 0.05 as the learning epoch progressed. The maximum learning epoch was limited at 5000. To find the optimal class number based on the fitness index defined in the previous section, a series of experiments varying the output node from 2 to 9 were executed. Table 2 and figure 10 shows the experimental results ; it indicates that the best classification performance was in the case of number 5. The table listed fitness values f_i for each class and its averaged value F for an examined number of output nodes varying from 2 to 9.

		Number of output node							
		2	3	4	5	6	7	8	9
class index	1	0.63	0.54	0.39	0.41	0.46	0.42	0.38	0.36
	2	0.30	0.34	0.34	0.40	0.47	0.45	0.32	0.33
	3	-	0.32	0.39	0.31	0.45	0.45	0.32	0.45
	4	-	-	0.35	0.32	0.40	0.36	0.37	0.34
	5	-	-	-	0.28	0.36	0.35	0.33	0.45
	6	-	-	-	-	0.34	0.40	0.46	0.34
	7	-	-	-	-	-	0.33	0.46	0.37
	8	-	-	-	-	-	-	0.40	0.31
	9	-	-	-	-	-	-	-	0.38
Averaged value		0.47	0.40	0.37	0.34	0.42	0.39	0.38	0.37

Table 2. Experimental result to determine the class number

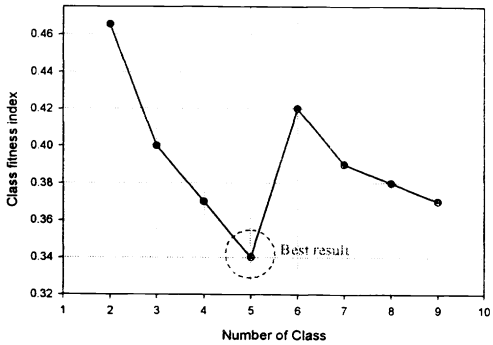

Figure 10. Choice of output node

Each final weight vector was labeled corresponding to its soldering quality by a human inspector. These weight vectors represent the classes, and are thus called prototypes. Figure 11 shows the prototypes of the trained LVQ neural network. The LVQ clustering neural network were used to distinguish solder joint profiles according to the variation between their shapes and generated prototypes. The prototypes were again categorized into 3 groups, which were insufficient, normal and excessive soldering profiles. Among the optimal five prototypes, two were for insufficient, another two were for excessive, while the other was for a normal soldering state.

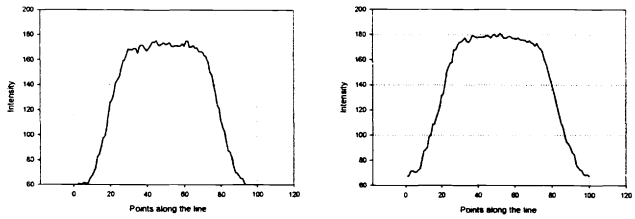

(a) Prototype of normal soldering (class 1, class 2)

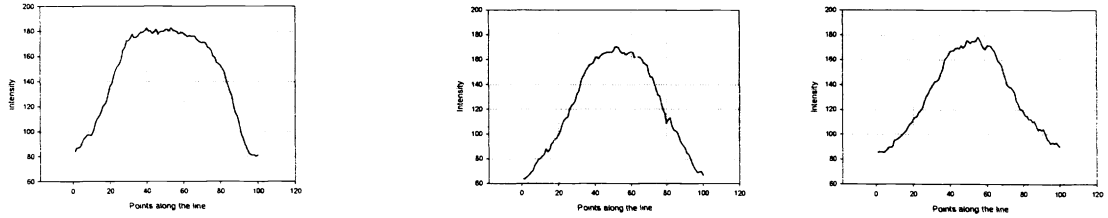

(b) Prototype of excessive soldering(class 3)

(c) Prototype of insufficient soldering(class 4, class5)

Figure 11. Prototypes of LVQ

4.3 Experiments for testing the LVQ network classifier

The LVQ neural network classifier was tested with another 232 profiles, called test samples, to check the validity of its classification results. For this purpose, the test samples were classified in advance by an human inspector, and then classified once again by the LVQ network.

		Normal		Excessive	Insufficient		Success
		class 1	class 2	class 3	class 4	class 5	rate (%)
Normal	class 1	**40**	2	0	*1*	0	93.0
	class 2	3	**73**	*3*	0	0	92.4
Excessive	class 3	0	0	**72**	0	*1*	98.6
Insufficient	class 4	0	*1*	0	**28**	2	90.3
	class 5	0	0	0	0	**6**	100.0

Table 3 . Classification result for test samples

Table 3 shows classification results for the test samples. The results appear to be satisfactory because the results between human classifier and the LVQ classifier were coincident. The success rate of the LVQ classifier was more than 90% ; and fortunately, most mis-classified samples yield correct results in the sense of quality groups, which were excessive, normal and insufficient. Among the 232 test samples, only 6 profiles classification results conflicted with each other. Thus, it can be said that the LVQ network has a confidence of 97.4% in deciding a solder joint quality.

In practice, in solder joint inspection, insufficient solder is a crucial defect because insufficient solder joints can crack easily under vibrations or shocks. For this reason, the success rate of the classification of insufficient defects should be close to 100% in designing the classifier. Our experimental results also show the high success rate for classification of insufficient solder joints, which implies that the classifier can be effectively used in actual application.

4.3 Building LUT(look up table) and BGA inspection results

For accurate inspection, four gray-level profiles on the lines passing through the center of a BGA solder joint in the x-ray image were considered together. The profiles were classified into one of the classes by the LVQ network, then the quality of the solder joint was judged based on the four classification results. In practice, the overall decision of a solder joint's acceptability is up to an human expert, and the rule can be built up as a lookup table. In this study, we concluded that if there are 3 or more coincident results, the result is adopted without doubt. But there can also be cases in which the profiles classifications show complementary results for a joint. For example, two directional profiles maybe insufficient, while the others are excess and normal solder. How can we conclude its inspection result for the cases? The LUT should be simple, but should also include all cases that are possible in the experiments ; thus it is built as shown in figure 12.

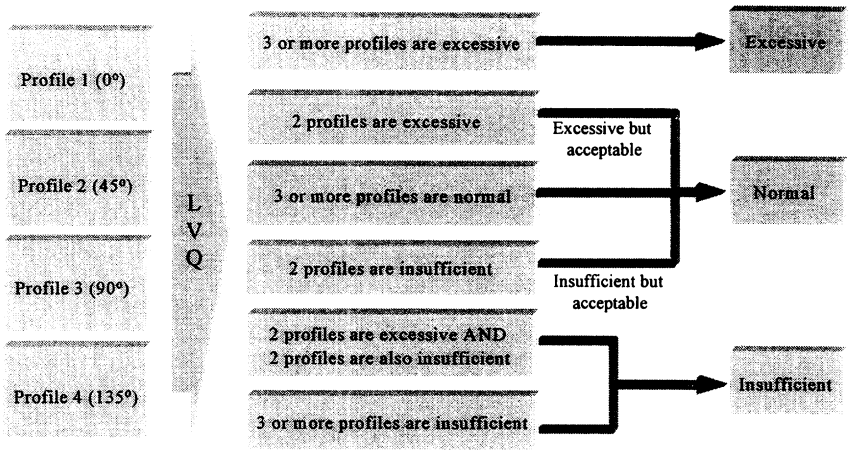

Figure 12. LUT(look up table) for BGA solder joint inspection

	Excessive	Normal			Insufficient
		Excessive but acceptable	Normal	Insufficient but acceptable	
number	10	17	29	8	4
Total(68)	10	54			4

Table 4. Experimental result for BGA solder joints

Table 4 shows experimental results for BGA solder joint inspection using the LVQ network and the LUT. In the experiment 68 BGA solder joints were examined ; 54 joints were found to show normal soldering, 10 and 4 joints were excessive and insufficient, respectively.

Figure 13 shows several examples of the experimental results for BGA solder joint inspection. The figures illustrate the DT images and their intensity distributions are expressed 3-dimensionally. The differences in the solder volume qualities could be easily discriminated by the naked eye and the proposed algorithm using the LVQ and LUT said the results correctly.

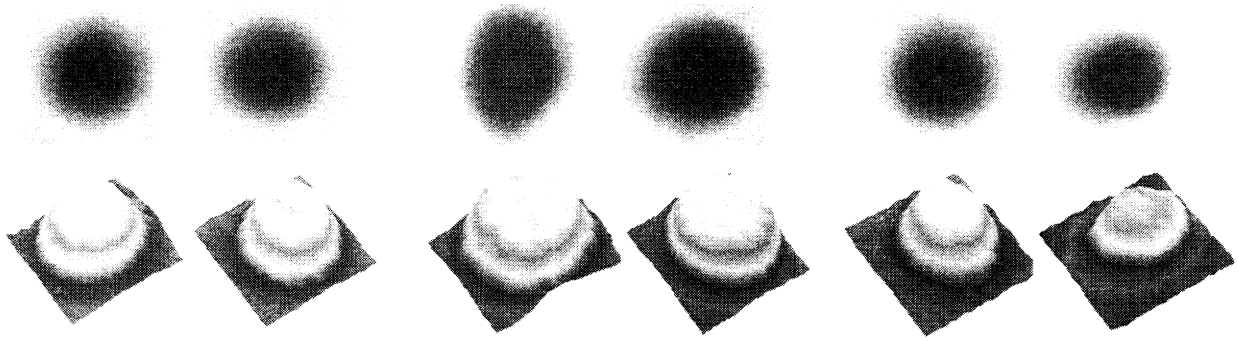

(a) Normal soldering (b) Excessive soldering (c) Insufficient soldering

Figure 13. Examples of BGA solder joints quality

5. Conclusions

In this paper, a series of algorithms for inspecting defects in BGA solder joints are proposed and their usefulness was verified by experiments on practical x-ray images acquired from the developed system.

Simple analysis on binarized images was applied to find out the defects such as location error or solder bridge between joints. However, to inspect solder volume in a joint, the intensity distribution in DT images was examined directly, and the distribution could be represented by four gray level profiles on the lines passing through the center of a joint. Considering the patterns of the profiles, the quality of the solder joints was determined to be either normal soldering or defective soldering (insufficient or excessive).

In this research, using a LVQ neural network and LUT approach is proposed to inspect and classify BGA solder joint quality. The LVQ neural network was trained with a number of teaching samples(profiles), and was able to classify input profiles into one of five classes representing solder joint quality. The number of classes(five in this case) was optimally determined from several experiments based on a fitness value describing the performance of the classifier. The LVQ network classification result had a success rate of more than 97% with respect to the results of human classifier.

To evaluate the classification performance of the proposed method, a series of experiments were conducted for a number of BGA solder joints on manufactured PCBs. The experimental results showed the practical usefulness of the proposed method for solder joint inspection.

ACKNOWLEDGEMENTS

This research was supported by Samsung Electronics Corporation and Korea government, and conducted through 1998~1999.

REFERENCES

1. S.T. Kang, Y.U. Kim and H.S. Cho, "A digital tomosynthesis method for evaluating the soldering states of ball-grid-array joints", 7th Annual Research Symposium of Transfer of Emerging NDE Technologies, 1998.
2. Adams, "X-ray laminography analysis of ultra fine pitch solder connections on ultra-thin boards", Integrated Circuit

Metrology, Inspection, and Process Control V (SPIE) Vol.1464. 1991, pp 484-497.
3. Black, D. L. Millard, and K.Nilson, "An animated interface for x-ray laminographic inspection of fine-pitch interconnect", IEMT Symposium 1991, pp 207-211.
4. M. Rooks, B. Benhabib, and K. C. Smith, "Development of an inspection process for ball-grid-array technology using scanned beam x-ray laminography", IEEE trans. on Components, Packing, and Manufacturing Technology - Part A. Vol. 18, No 4, December 1995. pp 851-861
5. Y.J. Roh, H.S. Cho, H.C. Kim, S.K. Kim, "Analysis of X-ray Image Qualities -Accuracy of Shape and Clearness of Image - Using X-ray Digital Tomosynthesis", Journal of ICASE (to appear), 1999.
6. S.T. Kang and H.S. Cho, "The Quality Evalution and Improvement for Digital Tomosynthesis Images", Materials Evaluation, 1998.
7. A. E. M. Bocage, "Laminographic imaging system for high energy radiation ", French Patent 536464(1922).
8. Y.J. Roh, Kuk Won Ko, H.S. Cho, H.C. Kim, H.N. Joo, "The calibration of x-ray digital tomosynthesis system including the compensation of the image distortion", Intelligent Systems and Advanced Manufacturing(SPIE), vol. 3528, 248-259, 1998.
9. Development of an PCB solder joints inspection system using x-ray, research report, Samsung electronics, 1997.
10. S.T.Kang, Arbitrary cross-sectional recognition of 3 dimensional objects using a digital tomosynthesis, Ph.D. thesis, Korea Advanced Institute of Science and Technology, 1998.
11. Jacek M. Zurada, "Introduction to Artificial Neural Systems", West Publishing company, 1992.
12. Y. Linde, et al., "An Algorithm for Vector Quantizer Design", IEEE Trans. On Communication, vol. com-28, no. 1, pp. 84-95, 1990.
13. Y.H. Pao, "Adaptive Pattern Recognition and Neural Networks", Addison-Wesley, pp 269-330, 1989.
14. D. H. Ballard, "Computer Vision", Prentice Hall, 1985.
15. Jurgen Schurmann, "Pattern Classification : A Unified view of statistical and neural approaches", A Wiley-Interscience Publication, 1996.
16. R.P. Lippmann, "Pattern Classification Using Neural Networks", IEEE, 1989.
17. S. T. Kang, H. S. Cho, "A projection method for reconstructing x-ray images of arbitrary cross-section", NDT & E International, vol.32. pp. 9-20, 1999.
18. S.T. Kang, J.H. Jeong, H.G. Song and H.S. Cho, "A new X-Ray cross-sectional imaging system for arbitrary angle inspection of BGA package", Proc. of NEPCON EAST '97, pp.109-120, 1997.